Chemisorption of benzene and STM dehydrogenation products on Cu(100)

N. Lorente*
Laboratoire Collisions, Agrégats, Réactivité, UMR 5589, IRSAMC, Université Paul Sabatier, 118 route de Narbonne, F-31062 Toulouse CEDEX 4, France

M. F. G. Hedouin and R. E. Palmer
Nanoscale Physics Research Laboratory, School of Physics and Astronomy, University of Birmingham, Edgbaston, Birmingham, B15 2TT, United Kingdom

M. Persson
Department of Applied Physics, Chalmers/Göteborg University, S-41296 Göteborg, Sweden
(Received 1 April 2003; revised manuscript received 9 July 2003; published 2 October 2003)

Modification of individual chemisorbed benzene molecules on Cu(100) has recently been performed in atomic manipulation experiments [J. Phys. Chem. A. **104**, 2463 (2000); Surf. Sci **451**, 219 (2000)]. Benzene dissociates under controlled voltage pulses in a scanning tunneling microscope (STM) junction. The reaction is characterized as a dehydrogenation process and the fragments are identified as benzyne, C_6H_4. Here we present a density functional theory investigation of the chemisorption of benzene on the Cu(100) surface, the nature of the bonding and its effect on the STM images. The fragments phenyl and benzyne formed after one-fold and two-fold dehydrogenation of chemisorbed benzene are studied in the same manner. The stability of the fragments is explored via their chemisorption energy, their electronic structure on the surface and their affinity for hydrogen. Benzyne fragments seem to be the most stable, in agreement with the conclusion of the aforementioned STM experiments.

DOI: 10.1103/PhysRevB.68.155401 PACS number(s): 68.43.Bc, 68.37.Ef, 73.20.Hb

I. INTRODUCTION

The adsorption of organic molecules on surfaces is of great interest from several different points of view. Indeed, much attention[2–5] is now given to the organic-inorganic interface, relevant to a wide range of applications, from the tuning of self-assembled monolayers to catalysis. In this paper, we report calculations of the chemisorption of benzene (C_6H_6), phenyl (C_6H_5), and benzyne (C_6H_4) on copper (100). This study is mainly motivated by a recent experimental study of single-molecule chemical reactions in the scanning tunneling microscope (STM).[1]

The chemisorption of benzene on various metallic substrates has attracted considerable attention recently. Theoretical studies of benzene on copper (110) and (111) surfaces[6–8] have been complementing experimental studies of these two surfaces.[9–14] Less work has been done on the (100) surface.[7] On the (111) and (100) surfaces it is generally concluded that benzene adsorbs with the aromatic ring parallel to the surface. This adsorption geometry suggests that the out-of-plane benzene π orbitals are mainly involved in the bonding process. Benzene chemisorption on transition metals has also been studied, as a model system for unsaturated hydrocarbon catalysis.[15] An example is the catalytic coupling of propyne on Cu(111), yielding benzene among other products.[16] Copper is a noble metal, with a full *d* band, thus reducing its reactivity as compared with Ni or other transition metals.[17,18] In relation to pure benzene, copper is quite inert,[19–21] and some theoretical work[7] concluded that the interaction is so small that benzene physisorbs on Cu(100).

The manipulation of benzene molecules on Cu(100) with the STM leads to the dissociation of benzene into smaller fragments.[1] The interpretation given[1] is that benzene undergoes a dehydrogenation reaction caused by the tunneling current. The symmetry and corrugation of the constant current STM images of the remaining fragments have been interpreted to indicate that benzyne is produced. Thus the removal of two hydrogen atoms from the benzene molecule appears to be more favorable than the removal of a single H. However singly dehydrogenated fragments are perfectly stable on noble metal surfaces. Phenyl fragments are found after iodobenzene dissociation on Cu(111).[22] Phenyl has been extensively studied on Cu surfaces.[23] The present work examines the nature of these two possible benzene dissociation fragments, i.e., phenyl and benzyne, created via STM dehydrogenation. Theoretical simulations allow us to check the experimental conclusions referring to the bonding, symmetry, and stability of the two different fragments on the surface. The study of the chemisorption and H affinities of the two different fragments provides a strong basis for identification of the fragments produced after atomic manipulation.

In Sec. II, we present the theory used in this work. Subsequently we explore the energetics, geometry, bonding and STM images of benzene on Cu(100). In Sec. III C we explore, in a similar way, the chemisorption of phenyl, and benzyne fragments of Cu(100). The discussion section (Sec. IV) addresses the comparison with published results on benzene chemisorption on Cu and Ni,[17–21] and the stability and nature of the chemisorbed fragments after dehydrogenation. Section V summarizes the conclusions of this work.

II. THEORY

In this section we give a short introduction to the theoretical method used. For a more complete description we suggest Refs. 24 and 25.

The density functional calculations of the free and chemisorbed molecule were carried out using a planewave, ultrasoft pseudopotential method as implemented by the codes DACAPO (Ref. 26) and VASP.[27,28] The exchange and correlation effects were described by a generalized gradient approximation. We used these two codes because the various codes developed to calculate the projected density of states (PDOS) and STM images were based on the Kohn-Sham wave functions generated by DACAPO, whereas the performance of VASP was exploited to find the equilibrium geometries of the systems. The Cu(100) surface was modeled by a four-layer slab and a vacuum region of five empty layers between the slab and its periodic images. The calculation of the STM images of an isolated molecule dictates the use of a rather large $p(4\times4)$ surface unit. The centers of the benzene molecule in this ordered structure are about 10.5 Å apart. We used a *k*-point set with 16 points in the surface Brillouin zone (SBZ). The change in energy when going from 9 to 16 *k* points was a few meV. The ultrasoft pseudopotentials allowed for kinetic energy cutoffs of 25 and 21 Ry in the plane-wave basis set for DACAPO and VASP, respectively. The ionic structure was relaxed until the various components of the force on each atom were less than 0.05 eV/Å. In finding the minimum energy configuration for the chemisorbed molecule, we allowed a full relaxation of the benzene molecule as well as a relaxation of the first two layers of copper. The binding energies obtained by these two codes agree within 0.05 eV. The study of the phenyl (C_6H_5) fragment was also performed with a five-layer vacuum gap, while for benzyne (C_6H_4) the vacuum gap was 12 layers. The phenyl and benzyne calculations were relaxed only to 0.1 eV/Å , due to the numerous degrees of freedom explored. The spin polarization of the electronic structure in all cases has been found to be zero. Hence the results presented in this work come from unpolarised calculations.

We have calculated the chemisorption energy, E_{chem}, as the difference between the total energy of the chemisorbed molecular system and the sum of the total energies of the free relaxed molecule and the surface. In the case of benzene on Cu(100), the chemisorption energy is then given by

$$E_{\mathrm{chem}}=E_{\mathrm{benzene/Cu(100)}}-E_{\mathrm{Cu(100)}}-E_{\mathrm{benzene}}. \tag{1}$$

Another calculated quantity is the hydrogen affinity, *A*. If we take as an example the formation of phenyl (C_6H_5), the H affinity is defined as

$$A=E_{\mathrm{(phenyl+H)/Cu(100)}}-E_{\mathrm{benzene/Cu(100)}}, \tag{2}$$

where $E_{\mathrm{phenyl+H/Cu(100)}}$ is the energy of the phenyl fragment plus a hydrogen atom separately chemisorbed on the surface. A positive affinity means that the energy balance favors the hydrogenated compound. We have not analyzed the dependence of the affinity on the H chemisorption site. In the reference experimental studies[1] the H atom likely ends up chemisorbed onto the STM tip.

Our analysis of the electronic structure and the bonding of benzene on Cu(100) was primarily based on an interpretation of the PDOS on molecular orbitals and also electron density differences. In a supercell geometry, the PDOS on a molecular orbital *a* is defined as

$$\rho_a(\epsilon)=\sum_{n,\mathbf{K}}|\langle\psi_{n\mathbf{K}}|\psi_{am\mathbf{K}}\rangle|^2\delta(\epsilon-\epsilon_{n\mathbf{K}}), \tag{3}$$

where $\psi_{n\mathbf{K}}(\mathbf{r})$ and $\epsilon_{n\mathbf{K}}$ are the Kohn-Sham wave functions and energies for the molecule chemisorbed on copper with band index *n* and wave vector **K** in the SBZ, and $\psi_{am\mathbf{K}}(\mathbf{r})$ are the corresponding wave functions in the same supercell for a free molecule, with the same geometrical configuration as the chemisorbed molecule, but for a single band *m*. To mimic the continuum of states of a semi-infinite substrate the delta function in Eq. (3) has been convolutioned with a Gaussian of 0.25 eV of broadening. The evaluation of the overlaps in Eq. (3) follows the procedure described in Ref. 24. The electron density difference is defined as the difference between the density of the chemisorbed molecule and the superposition of the densities of the free molecule and the bare substrate.[29,30]

We calculated the STM images using the Tersoff-Hamann theory[31,32] and Kohn-Sham wave functions and energies of the chemisorbed molecule. This theory is based on an *s*-wave approximation for the tip and gives (at zero temperature and low tip-sample bias) a tunneling conductance that is proportional to the local density of states (LDOS), $\rho(\mathbf{r_0},\epsilon_F)$, at the Fermi level ϵ_F and the position $\mathbf{r}_0$ of the tip apex (curvature center of the extremity of the tip). Thus constant-current STM images correspond in this theory to constant LDOS images. In a supercell geometry, this LDOS $\rho(\mathbf{r_0},\epsilon_F)$, obtained using the Kohn-Sham states and energies of the chemisorbed system, is given by

$$\rho(\mathbf{r_0},\epsilon_F)=\sum_{n\mathbf{K}}|\psi_{\mathbf{nK}}(\mathbf{r}_0)|^2\delta(\epsilon_F-\epsilon_{n\mathbf{K}}). \tag{4}$$

The procedure used to evaluate the ultrasoft pseudo-wave-functions at the tip apex in the remote vacuum region is described in Ref. 24. The continuum of states of a semi-infinite substrate is mimicked in the same manner as for the PDOS. We have also analyzed the additive contributions, $\rho_{n\mathbf{K}}(\mathbf{r_0},\epsilon_F)=|\psi_{\mathbf{nK}}(\mathbf{r}_0)|^2\delta(\epsilon_F-\epsilon_{n\mathbf{K}})$, from each Kohn-Sham state to $\rho(\mathbf{r}_0,\epsilon_F)$.

III. RESULTS

In this section we present the calculated electronic structure for benzene (C_6H_6), phenyl (C_6H_5), and benzyne (C_6H_4) on Cu(100). The electronic structure of the chemisorbed molecules can be rationalized in terms of the electronic structure of the free molecule and of the surface.[18]

A. Benzene on Cu(100)

The most favorable adsorption site of C_6H_6 on Cu(100) is the hollow one, with a chemisorption energy of -0.68 eV, followed by the bridge site, -0.47 eV, and then the top site,

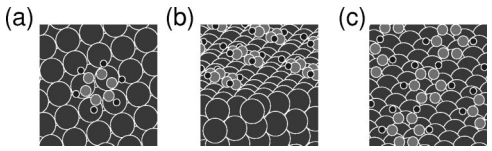

FIG. 1. Schemes of benzene (a), phenyl (b), and benzyne (c) chemisorbed on Cu(100). Different perspectives are given for each case in order to emphasize the different bondings. Benzene (a) chemisorbs flat on the hollow site of the (100) surface. Phenyl (b) chemisorbs at an angle with the unpair C bonding onto the top site. Benzyne (c) stands up on the hollow site.

−0.38 eV. Benzene adsorbs with its center of gravity over the hollow position; see Fig. 1(a). The carbon ring remains parallel to the surface at a height d_z of 2.23 Å. Four carbon atoms are near the first-layer copper atoms (2.35 Å), and the two remaining atoms are sitting on bridge positions 2.74 Å away from the copper atoms. The adsorption also induces an expansion of the carbon ring as compared to the free molecule. The C-C distance expands from 1.398 Å to 1.414 or 1.420 Å, depending on the location of the pair of C atoms. We also notice that the H atoms are lying approximately in the same plane as the benzene ring; however they are in fact slightly tilted away from the surface by about 8°. Looking at the substrate we remark that the four copper atoms lying beneath the benzene ring elongate horizontally to 2.630 Å, which represents 2% of the relaxed lattice parameter, and vertically buckle away from the surface by 0.08 Å, a change of 4%. To sum up, the adsorption of benzene on Cu(100) induces slight geometrical distortions of both the adsorbate and surface. These results are in good agreement with the cluster calculations of Pettersson *et al.*[7]

We analyze the electronic structure of the C_6H_6/Cu (100) system in terms of the electronic structure of both the free molecule and the free surface. This analysis allows us to understand the bonding of benzene to Cu(100), as well as the STM images presented in Sec. III B. Yamagishi *et al.*[18] gave a clear explanation of benzene bonding on Ni(111) in terms of the frontier molecular orbitals [highest occupied molecular orbital (HOMO) and lowest unoccupied molecular orbital (LUMO)], similar to the approach we present here.

The slight geometrical distortions upon adsorption of the molecule make it possible to describe the molecular orbitals of the free, distorted molecule with the same notation as for the free undistorted molecule. These distortions reduce the symmetry of the free molecule from D_{6h} to C_{2v}, which in turn lifts the degeneracy of molecular orbitals with E character and makes hybridization between some orbitals of different symmetry character with respect to D_{6h} symmetry allowed. However, for the molecular orbitals of interest here we find that the perturbations on these orbitals are weak and that they keep their character. We find that the shifts and mixings of the energy levels of these molecular orbitals are small.

In Fig. 2(a), we show the calculated PDOS for the chemisorbed molecule onto some occupied molecular orbitals of the free, distorted molecule. We have only projected onto molecular orbitals which are resonant with the copper conduction band, namely, the π complex comprising the $1a_{2u}$

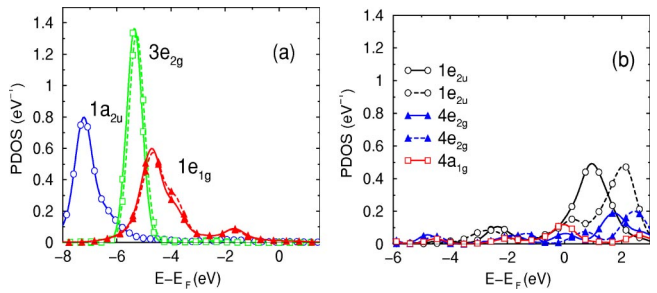

FIG. 2. (Color online) Projected density of states (PDOS) of the full C_6H_6/Cu(100) system on free-molecule orbitals. The site is hollow. The molecule has a C_{2v} symmetry, but we have kept the free-molecule symmetry notation D_{6h}. In (a) we have plotted the PDOS onto occupied free-molecule orbitals. In (b) the PDOS corresponds to the unoccupied free-molecule orbitals. In every PDOS calculation we have used 16 k points in a 4×4 supercell, as in the chemisorption and STM calculation.

MO and the two $1e_{1g}$ MOs and the σ orbitals (the $3e_{2g}$ MOs). We find that the lower-lying σ orbitals interact weakly with the Cu states. The single peak in the PDOS for the $3e_{2g}$ orbitals (their natural width cannot be resolved) shows that the interactions with the copper conduction band are weak. The $1a_{2u}$ orbital and the two $1e_{1g}$ orbitals interact strongly with the copper conduction band, leading to a substantial broadening and shift of the original states relative to the peak derived from the $1e_{1g}$ orbital. The secondary peak in the PDOS for the $1e_{1g}$ orbitals is in the same energy range as the d band of copper, and shows that these orbitals hybridize substantially with the d states of copper. Note that the splitting of the twofold degenerate orbitals are negligible.

In Fig. 2(b), we show the calculated PDOS for the chemisorbed molecule for the lower-lying unoccupied molecular orbitals of the free, distorted molecule. All these molecular orbitals interact strongly with the copper conduction band, as is evident from their large broadening. The large broadening comes from the interaction with the sp conduction band. In particular, the $1e_{2u}$ orbitals are considerably modified by the interaction with the substrate. As a result, their degeneracy is broken with a splitting of about 2 eV, to be compared with the splitting of 0.05 eV for the free, distorted molecule. These orbitals generate long tails below the Fermi level, are partially occupied, and hybridize with the copper d states. This back donation is dominated by electron transfer to the $1e_{2u}$ orbitals.

The electron transfer to the LUMO of the C_6H_6 molecule is in apparent disagreement with the calculated reduction of about 0.6 eV in the work function upon adsorption.[20,33,34] An electron transfer suggests an increase of the magnitude of the surface dipole, resulting in an increase of the work function. However, the laterally integrated electron density difference depicted in Fig. 3 shows not only the electron transfer but also a large reduction of the electron density just above the molecule. This reduction results in a net positive dipole moment due to the charge redistribution and a reduction of the work function. These results show that it is the rearrangement of charge about the molecule the cause of the work function change.

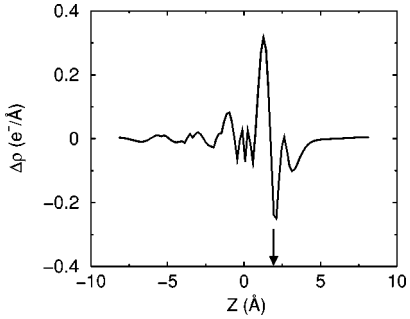

FIG. 3. Induced density laterally integrated in units of electrons per Å. $Z=0$ corresponds to the topmost surface layer and negative values indicate the bulk direction. The vacuum side is the positive one. There is a pileup of negative charge (here a positive number of induced electrons) between the molecule and the surface. The molecule center lies 1.93 Å from the topmost surface layer (arrow). The induced dipole is thus positive, leading to a reduction of the surface work function.

We find that the trend in the chemisorption energy among the high symmetry sites correlates with the back donation to the LUMO.[35,36] In Figs. 6(a) and 6(b) we show the calculated PDOSs of the chemisorbed molecule in the top and bridge adsorption site, respectively, for the relevant π and π^* orbitals of the free, distorted molecule. As can be seen from Figs. 2 and 6, the trend is an overall downward shift in energy of the states derived from these orbitals, which is largest for the hollow site and smallest for the top site. This trend is related to the degree of overlap of these orbitals with the copper *d* states for the different adsorption sites. For all sites the states derived from the π orbitals are essentially fully occupied and give a small contribution to the bonding, whereas the partial occupation of states derived from the $1e_{2u}$ degenerate orbitals is substantial, making a large contribution to the bonding. The back donations to the $1e_{2u}$ orbitals are about 0.9, 0.56, and 0.2 electrons for the hollow, bridge, and top sites. This trend correlates well with the trend of binding energies.

B. STM images of C_6H_6/Cu (100)

In this section we present our calculated constant current STM images of the chemisorbed molecule, and discuss them in terms of the calculated electronic structure and the experimentally observed image. These images have been calculated using the Tersoff-Hamann theory described in Sec. II.

In Fig. 4(c), we show the contours of the constant local density of states $\rho(\mathbf{r}_0,\epsilon_F)$ evaluated at the tip apex $\mathbf{r}_0$ for the chemisorbed molecule on the hollow site. As we shall discuss later, we have chosen a value for $\rho(\mathbf{r}_0,\epsilon_F)$ that reproduces the observed corrugation height in a constant current STM image. We find that the topography of this image, that is, a single protrusion with a C_{4v}-like symmetry, does not change qualitatively for different values of $\rho(\mathbf{r}_0,\epsilon_F)$. However, there are some quantitative changes in the topography; both the corrugation and the lateral extent of the protrusion change with the tip-surface distance. The protrusion has a much larger spatial extent than the molecule itself, and shows the need to use a large surface unit cell for the calculation of an STM image from an isolated chemisorbed molecule. The artifact of representing a single molecule with a $p(4\times4)$ overlayer of molecules becomes noticeable through a relative increase of the corrugation between the molecule and its periodic images when the tip-surface distance is comparable to a surface unit cell size of about 10 Å. For the other adsorption sites, we also find a single protrusion with no nodal planes in the calculated STM image. It is only for the bridge site that the C_{2v} symmetry of the adsorption site can be discerned in the image, whereas for hollow and top sites the images seem to have higher symmetries than the adsorption site.

The topography of the calculated STM image can be readily understood from the behavior of the PDOS for the molecular orbitals at the Fermi level as well as the spatial character of these orbitals in the lateral direction. In order for the electronic states that derive from a molecular orbital to contribute to $\rho(\mathbf{r}_0,\epsilon_F)$, the PDOS on that molecular orbital has to have a substantial contribution at the Fermi level and the orbital must also have a relatively slow decay into the vacuum region where the tip apex is located. This decay is governed by the kinetic energy of the lateral components of

TABLE I. Chemisorption energy on Cu(100), E_{chem}, and hydrogen affinity A for C_6H_6, C_6H_5, and C_6H_4. Equations (1) and (2) give the definitions of the adsorption energy and the hydrogen affinity. A positive affinity means that the system reduces its energy if the molecule bonds to an extra hydrogen atom. For comparison we reproduce the same values for the corresponding acetylene series, C_2H_2, C_2H, and C_2, published in Ref. 25.

	C_6H_6	C_6H_5	C_6H_4
E_{chem} (eV)	−0.68	−2.59	−3.52
A (eV)		1.56	0.84
	C_2H_2	C_2H	C_2
E_{chem} (eV)	−1.31	−4.22	−6.57
A (eV)		0.58	0.82

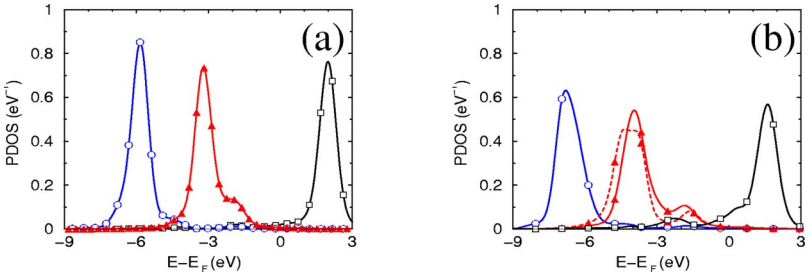

FIG. 6. (Color online) PDOS onto free-molecule orbitals for top (a) and bridge (b) sites. The tails corresponding to the $1e_{2u}$ (a_2 in C_{2v}) state account for the back-donation. The back-donation is bigger for the bridge case. The $1a_{2u}$ PDOS is partially hybridized with the *d* band in the top case, becoming larger than the $1a_{2u}$-PDOS of the bridge case.

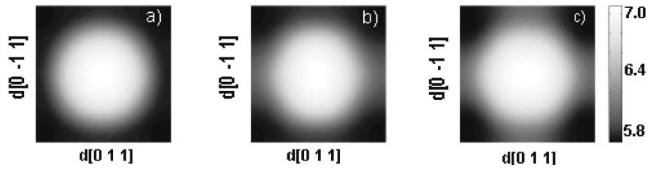

FIG. 4. Constant current images of a benzene molecule chemisorbed on (a) the top site, (b) the bridge site along the [011] direction, and (c) the hollow site. Analysis of these images, in terms of individual electronic states, permits us to assign the particular site dependence to the PDOS presented in Figs. 2 and 6.

the plane waves that build up this orbital, which favors orbitals with the smallest lateral spatial variation. In particular, states with the fewest number of nodal planes, as provided by the totally symmetric orbitals, will have the slowest decay into the vacuum region. In this case, the $4a_{1g}$ orbital is totally symmetric and its PDOS is as large as the LUMO PDOS at the Fermi level, as shown in Fig. 2. Thus states that derive from this orbital should give a dominant contribution to the STM image. This explains why the image consists of a single protrusion with no nodal planes.

The conclusion that the protrusion is derived from the $4a_{1g}$ orbital is confirmed by an analysis of the additive contributions from different Kohn-Sham states to $\rho(\mathbf{r}_0,\epsilon_F)$. In Fig. 5, we have plotted the contributions $\rho_{n\mathbf{K}}(\mathbf{r}_0,\epsilon_F)$ from all Kohn-Sham states (with band index n) at the $\bar{\Gamma}$ point within an energy range of 0.25 eV from the Fermi level. As can be seen in Fig. 5, $\rho_{n\mathbf{K}}(\mathbf{r}_0,\epsilon_F)$ in (a) and (e), with zero nodal planes, give the dominant contributions. The corresponding states overlap with the $4a_{1g}$ orbital. The $\rho_{n\mathbf{K}}(\mathbf{r}_0,\epsilon_F)$ contribution in (d), with two nodal planes, is smaller by a factor 4 (note the different vertical scale). The corresponding state has a large overlap with the free-molecule LUMO orbital, $1e_{2u}$. Finally, the $\rho_{n\mathbf{K}}(\mathbf{r}_0,\epsilon_F)$ contributions in (b) and (c) are smaller by three orders of magnitude. Thus the analysis confirms that the protrusion arises from states that derive from the $4a_{1g}$ orbital, at least within the Tersoff-Hamann approximation.

Weiss and Eigler[37] demonstrated the chemisorption site dependence of the STM image of C_6H_6/Pt(111). This site dependence is particularly important on semiconductor surfaces, where the molecular geometry is strongly perturbed by the adsorption process.[38] On metallic surfaces, Sautet and Bocquet[39] explained this dependence by studying the modification of the molecular orbitals at different chemisorption sites. Our approach allows an association of the STM image with the PDOS at the Fermi level. In agreement with previous work, the calculated PDOS at the Fermi level (Fig. 6) and the calculated STM image (Fig. 4) show a site dependence. Chemisorption at the bridge site gives images with a C_{2v}-like symmetry; the image is elongated perpendicular to the two H atoms coinciding with Cu substrate atoms in the [011] direction. Meanwhile, the top-site image shows a high symmetry with no preferential direction. The LDOS decomposition permits us to understand the site-dependent image in terms of the MOs of benzene. At the hollow site, the $1e_{2u}$ (LUMO) degeneracy is lifted and the image reflects the two nodal planes of the LUMO. As we explained in Sec. III A, the one-electron structure is shifted upwards on the top and bridge sites. The contribution of the LUMO to the STM images on both sites is reduced, where the contribution of the HOMO is increased, as compared with the hollow site case. Figure 6(a) shows that for the top site the two $1e_{2g}$ (HOMO) are totally degenerate while the degeneracy is lifted at the bridge site. Hence, at the top site the STM image presents the contribution of both $1e_{2g}$ orbitals: this gives a totally symmetric image. Nevertheless, the contribution from a_1-like orbitals is still the largest. At the bridge site, the degeneracy is lifted [Fig. 6(b)], and only one of the $1e_{2g}$ orbitals contributes to the STM image. This orbital presents a nodal plane along the [011] direction. The corresponding image is fairly symmetric because of the dominating a_1 orbitals, but does become elongated along the $1e_{2g}$ direction.

To conclude, the calculated STM image is in good agreement with the observed constant-current image of C_6H_6 adsorbed on Cu(100)[1]. The observed image shows a single protrusion with a height of 1 Å and an overall width of about 7 Å, with a fourfold rotation axis symmetry, which is nicely reproduced by the calculated image at an average tip-surface distance of 5.7 Å away from the molecule.

C. Dehydrogenation fragments

The aim of the work reported in this section was to study the two chemisorbed fragments of benzene, i.e., phenyl (C_6H_5) and benzyne (C_6H_4), obtained by the removal of one or two H atoms. The phenyl (C_6H_5) fragment was found to chemisorb with the C ring forming an angle of 20° with the surface; see Fig. 1(b). The C atom without a H is closest to the surface and the phenyl ring folds slightly about the mirror plane perpendicular to the surface which contains the unsaturated carbon atom. The phenyl fragment thus presents

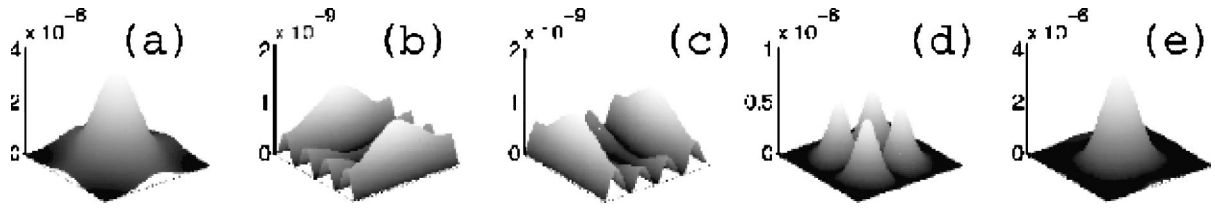

FIG. 5. Three-dimensional plots of the contributions, $\rho_{n\vec{K}}(\vec{r}_0,\epsilon_F)$, from individual Kohn-Sham states to the local density of states $\rho_{n\vec{K}}(\vec{r}_0,\epsilon_F)$ at the Fermi level. (a)–(e) are all the states within 0.25 eV from the Fermi level and at the $\bar{\Gamma}$-point ($\vec{K}=0$) (a) and (e) correspond to states of symmetry a_1 belonging to the C_{2v} point group, whereas (b) and (c) correspond to eigenstates that contain no contribution of molecular states. (d) is the symmetry a_2 part of the contribution of the lowest unoccupied molecular orbital $1e_{2u}$ at the Fermi level.

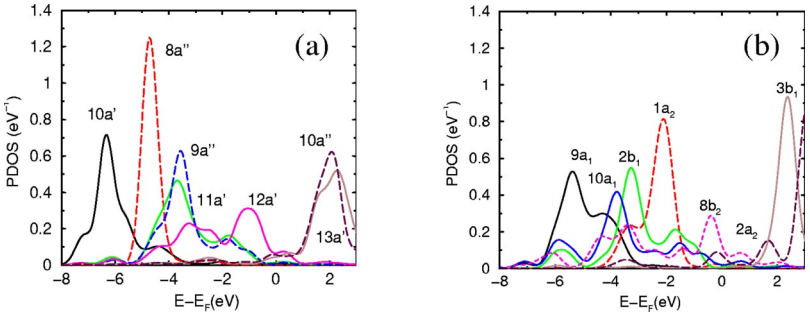

FIG. 7. (Color online) Projected density of states (PDOS) for C_6H_5 in (a) and C_6H_4 in (b) chemisorbed on Cu(100). Dashed lines denote the density of states projected on molecular orbitals with a nodal plane perpendicular to the C ring.

a *quasi-*C_s symmetry on the surface. The unpaired C lies close to a Cu atom and the phenyl fragment can basically turn about the axis perpendicular to the surface on this Cu atom. As a consequence the chemisorption energy of phenyl with the C ring over the hollow site is -2.59 eV, while the chemisorption energy with the C ring over a bridge site is -2.56 eV. The atop configuration (where the C ring is vertical) is not favored, with a chemisorption energy of -1.39 eV. The H affinity of the C_6H_5 fragment is $A=1.56$ eV when chemisorbed on Cu(100).

Benzyne, C_6H_4, chemisorbs through its two unsaturated C atoms; the C ring is vertical, see Fig. 1(c). It has two mirror planes and thus its symmetry belongs to the C_{2v} point group. The preferred chemisorption site is the hollow site, with a chemisorption energy of -3.52 eV. The ring lies along the $[1\bar{1}0]$ axis. It is possible that this result is coverage dependent. We have checked that the direct interaction between free benzyne molecules is negligible in the present $p(4\times4)$ structure, but substrate-mediated interactions may play a rôle. We have also found a metastable state in which the C ring is tilted by 46° with respect to the surface plane. The chemisorption energy for this intermediate geometry is -3.27 eV. The value of the hydrogen affinity is 0.84 eV.

It is interesting to compare the electronic structure of the two benzene fragments. As in the case of benzene, the chemisorption of phenyl and benzyne are largely dominated by electron donation from the metal surface into the LUMO. The donation is large enough to equilibrate the spin polarization of the free phenyl molecule once it is chemisorbed, so that the spin polarization disappears. The highest occupied benzene orbital that involves the bonding of H atoms is the $3e_{2g}$ state of benzene. As a H atom is separated from the benzene molecule, the $3e_{2g}$ state shifts upwards in energy, becoming the half occupied molecular orbital $12a'$ of phenyl. In the case of benzyne, both $3e_{2g}$ benzene states evolve into the HOMO, $10a_1$, and LUMO, $8b_2$.

The projected density of states as defined in Eq. (3) is shown in Fig. 7 for (a) C_6H_5 and (b) C_6H_4 chemisorbed on Cu(100). In phenyl, the LUMO $12a'$ becomes occupied upon chemisorption, as can be seen in Fig. 7(a). The other $3e_{2g}$ state becomes the $8a''$ orbital. The binding of phenyl proceeds through substrate donation into the $12a'$, forming a σ-like bonding. The chemisorption geometry of phenyl arises from the competition between the σ-like bonding to the surface of the LUMO $12a'$ and the π-like bonding involving orbitals $11a'$, $13a'$, $9a''$, and $10a''$. The σ bonding interaction tends to cause the C ring to stand perpendicular to the surface, while the π bonding tries to optimize the overlap with the substrate, pushing the C ring parallel to the surface. As a result, the molecule is tilted.

The removal of a second H atom from benzene to create benzyne changes the bond picture. The LUMO basically captures two electrons from the surface, and the π overlap with surface states is greatly reduced. The molecule presents a vertical C ring. The bonding is directed by the two unsaturated C atoms, and both the symmetry of the LUMO and the induced charge are reminiscent of acetylene bonding on Cu(100).[25]

D. STM images of C_6H_5 and C_6H_4 on Cu(100)

The calculated STM constant-current images of phenyl and benzyne on Cu(100) both show planar symmetries, in accordance with the molecular symmetry: C_s-like for phenyl, and C_{2v}-like for benzyne. But the two images are rather similar. The only important difference is the corrugation. Benzyne presents $\sim$0.5-Å higher corrugation than phenyl because its C ring is perpendicular to the surface plane. Only when the simulation is carried out very near to the surface does the C_{2v}-like benzyne become distinct from the phenyl case. Constant-current images may thus be insufficient to enable the identification of the fragment formed experimentally.

The molecular-orbital origin of the STM images of the fragments reflects the prevailing σ bonding in both cases. In both fragments the responsible LUMO shows nodal planes perpendicular to the C ring that would image as depressions in the STM. Hence, despite the perturbation caused by the distortion of the molecule and the new electronic structure near the Fermi level, the origin of the STM image of phenyl is similar to that of benzene and due to an unoccupied highly symmetrical molecular orbital over the C ring (i.e., the orbital $4a_{1g}$ of benzene). On Cu(111), phenyl images are totally symmetric, with a close resemblance to benzene.[22] Benzyne stands up on Cu(100), and the unoccupied *a*-like orbitals are π-like over the C ring: this means that a nodal plane coincides with the C-ring plane. This is not what is seen in the calculated STM image. The electronic structure originating in the HOMO is totally symmetric about the C-ring plane. Hence, the STM image presents features reflecting the HOMO, contrary to phenyl and benzene. The reason why the HOMO contributes in benzyne and not in phenyl and benzene is twofold: (i) phenyl and benzene are largely planar, hence nodal planes about the C ring will not affect the STM image; and (ii) the absence of the two hydro-

gens shifts the σ-like orbitals towards the Fermi level, hence the benzyne HOMO presents no nodal plane about the C ring which is now vertical. The electronic structure originating in MOs without nodal planes will yield a larger contribution to the LDOS, and hence to the STM image, as shown here.

E. Hydrogen affinity and fragment stability

Table I shows the chemisorption energy for benzene, phenyl, and benzyne, as well as the hydrogen affinity for the two fragments. It is instructive to compare these values with those obtained for the acetylene series.[25] In both series, the chemisorption energy increases with the degree of dehydrogenation since the degree of surface bonding increases. The hydrogen affinity A is positive because the hydrogenated chemisorbed molecule is energetically more favorable. As compared with the gas-phase values, A is much smaller on the surface because the fragment is partially saturated by the surface and because the freed H atom is chemisorbed. As the degree of dehydrogenation increases, A increases for the acetylene series, but it diminishes for the benzene fragments. This is a remarkable difference in behavior between the two series. Benzyne adsorbs more strongly than phenyl and its bonds are almost saturated by the surface, so its affinity for hydrogen is a factor 2 smaller than in the phenyl case. This is an indication of the greater stability of chemisorbed benzyne as compared with the phenyl fragment on copper.

IV. DISCUSSION

In this section we discuss our results for the geometric and electronic structure (and STM images) of benzene and its fragments on Cu(100) in relation to results obtained by other electronic structure calculations and experimental data for adsorption on metal surfaces. The hollow adsorption site and the planar configuration of the molecule (with the canting of the H atoms) is generally found in experimental studies of benzene adsorption on metal surfaces.[9–14] This geometric configuration is characteristic of bonding via the π-π^* complex of molecular orbitals.

The relative participation of these orbitals (i.e., π vs. π^*) to the bonding is found to be specific to the metal surface. Our conclusion that the bonding is predominantly through electron donation to the π^* molecular orbitals, and that chemisorption is weak on copper, was also obtained in the density functional calculations for the chemisorbed molecule on Cu(100) (Ref. 7) and Cu(110) (Ref. 20) surfaces. In the density functional calculations by Mittendorfer and Hafner,[17] using a slab model for the C_6H_6 chemisorption on the (100), (111), and (110) surfaces of Ni, they found the chemisorption energy to be about 1.5 eV larger than on Cu, while the molecule was closer to the surface by about 0.3 Å and the C-C distance elongated by 0.03 Å on the Ni(100) surface.

As pointed out by Weinelt *et al.*,[20] the stronger chemisorption bond and perturbation of the molecule by Ni than by Cu can be understood in terms of the more active role of the highest occupied π orbitals $1e_{1g}$ and the partially occupied d states of Ni than on Cu (where the d states are fully occupied and lower in energy). In particular, the interaction of these π molecular orbitals with the higher-lying d states of Ni than on Cu results in a substantial back donation.

This conclusion about the importance of the position of the d states in the bonding of benzene to metal surfaces is supported by Koschel *et al.*[21] in their experimental study of benzene adsorption on Ni(111) and Cu/Ni(111). They used temperature programmed desorption and angle-resolved ultraviolet photoelectron spectroscopy to explore the strength of the adsorption and the shift of the molecular levels upon chemisorption. Their results showed that a single Cu layer on Ni(111) changed the reactivity of the Ni surface from strong chemisorption and large level shifts to weak chemisorption and small level shifts, as typical of Cu.

As a consequence of charge transfer and surface screening, we find a large depletion of electrons in the vacuum region [negative values of $\Delta\rho(Z)$] and a large concentration of electrons between the molecule and the surface. Thus the total induced dipole is positive, leading to a reduction of the work function. This result is similar to the analysis of Held *et al.*[40] concerning the work function reduction for benzene adsorption on Ru(0001). They argued that despite the back-donation evaluated in their calculation, their calculated work function shift is due to the total positive induced dipole caused by the charge counterbalance of the top two substrate layers,[40] analogous to our Fig. 3. The change of the work function has its origin in the rearrangement of charges about the molecule rather than in the ill-defined total charge transfer.

There have been a very limited number of calculations of STM images for chemisorbed molecules based on density functional calculations, because these calculations, require a large surface unit cell to represent the image, as well as the somewhat controversial Tersoff-Hamann approximations for the tunneling current and the tip. However, the calculations using this approach for C_2H_2 on Cu(100) have shown that it gives a good account of the observed images, in particular for the images recorded by a functionalised tip.[25] Prior to this work, to our knowledge, there have been no reports of density functional calculations of STM images for benzene on a metal surface. The only results that have been reported so far were obtained for benzene on Pt(111) using extended Hückel calculations and a Landauer approach for the tunneling that is more sophisticated than the Tersoff-Hamann approximation.[39]

Finally, it is worth noting that, as in previous reports,[37,39] we find a site dependence of the STM image. The image reflects, to some extent, the symmetry of the chemisorption site, which is a consequence of the rehybridization of the $4a_{1g}$ state with the states of the different neighboring substrate atoms. On other substrates, the balance of the molecular orbitals at the Fermi level will certainly change, as is the case for Pt (111) (Refs. 37 and 39) or Ag(110).[41]

The chemisorption of benzene fragments of the type that might be formed by STM dehydrogenation can be understood quite easily. The chemisorption energy increases at increasing stages of dehydrogenation because of the more unsaturated character of the new molecular bonds. This is same the trend found in the acetylene dehydrogenation series.[25] In the cases we have considered (i.e., phenyl and benzyne) the

H affinity is positive, meaning that the system prefers full hydrogenation on Cu(100), because the surface bonding is not sufficient to saturate the molecular bonds of the adsorbate species.

The present dehydrogenation process which occurs during STM dissociation is not clear yet. Lauhon and Ho[1] show that the dissociation reaction takes place at a tip-sample bias of 2.9 V. In the case of deuterated benzene, dissociation takes place at 4.4 V. The occurrence of this threshold behavior is not consistent with a vibrational mediated process. Instead, as suggested in the case of the dehydrogenation of a silicon surface,[42] the initial excitation mechanism seems to be electronic in nature. Hence the electronic structure of the chemisorbed molecule must influence the dissociation process.[43] As shown by the isotopic effect, the actual dissociation bias will depend on the complicated dynamics of the dissociation process. Heavier atoms move more slowly and since the system can de-excite before dissociation[44] more energy must be conveyed by the impinging electron.

Lauhon and Ho[1] concluded that benzyne fragments are formed after studying the constant current STM image and the inelastic electron tunneling (IETS-STM) spectrum. The experimental constant current STM image presents a C_{2v} symmetry, of the type that a standing up benzyne fragment would show. The C-H stretch mode is not detectable for benzene. However, after STM manipulation a C-H stretch mode becomes detectable. Lauhon and Ho argues that C-H bonds sticking out of the surface would be more easily detectable by IETS-STM. Hence benzyne the most likely fragment in the experimental reaction induced by the STM is benzyne.

Weiss *et al.*[22] have shown that phenyl fragments chemisorbed on Cu(111) show a cylindrical symmetry, similar to chemisorbed benzene molecules. Our STM simulations show that constant-current images of phenyl and benzyne present certain similarities. STM images of phenyl fragments centered on the bridge site of Cu(100) present a C_{2v} symmetry. Hence the symmetry of the constant-current image may not be enough to determine the identity of the fragment. Moreover, in phenyl C-H bonds can also point away from the surface so that IETS-STM detection of C-H based modes form phenyl cannot be ruled out.

These facts give a special value to the calculations presented. The hydrogen affinity drops by a factor of 2 for benzyne as compared to phenyl. On the other hand, benzyne presents a chemisorption energy larger than the phenyl fragment. The stability of benzyne on the copper surface is greater in two senses: it is more strongly bound to the surface, and it gains less energy than phenyl in the hydrogenation process. The study of the energy balance in the chemisorption of benzyne and phenyl shows that benzyne is more stable than phenyl on Cu(100), and hence more likely to be the fragment created in the STM experiments.

V. CONCLUSIONS

In this paper, we have described density functional calculations of the chemisorption and STM images of benzene on the (100) face of a copper surface. The calculations are based on a plane wave, ultrasoft pseudopotential method using a slab model of the copper surface and a $p(4\times4)$ ordered overlayer to represent the isolated molecule. The STM image has been calculated using the Tersoff-Hamann approximation and the Kohn-Sham states of the benzene-covered surface.

We find that benzene is weakly chemisorbed and that the hollow site is the most favourable adsorption site amongst the high symmetry sites. The molecule is adsorbed in a planar configuration with a slight tilting of the H atoms away from the carbon ring. This adsorption site is in agreement with results from scanning tunneling microscopy experiments. The planar configuration is supported by the good agreement of the calculated STM image with the observed image. Our qualitative analysis of the bonding in terms of the projected density of states suggests that the bond is formed predominantly by donation of electrons to the lowest-lying π^* orbitals of the molecule, which interact strongly with the *sp* bands of copper. In particular, we find that the hollow site gives rise to the largest charge donation to these orbitals, which makes the hollow site the most stable site. The bonding π orbitals of the molecule are found to hybridize strongly with the *d* and p_z orbitals of the copper atoms. However, this does not give rise to any substantial donation of electrons to the copper surface, which has a fully occupied *d* band, in contrast to what has been found for other transition metal surfaces with partially occupied *d* bands. Donation to the unoccupied *sp* conduction band is very small due to the large energy mismatch between the HOMO peak and the Fermi energy.

The calculated STM image, exhibiting a single and symmetric protrusion, cannot be rationalized in terms of tunneling through states derived from the LUMO. Instead, we find that states derived from a totally symmetric, unoccupied σ orbital of the molecule give the dominant contribution to the STM image. In general, we expect that states derived from those molecular orbitals with the least number of nodes along the surface and which give the most substantial contributions to the PDOS at the Fermi level should determine the shape of the STM image at a low tip-surface bias.

The dehydrogenation fragments phenyl (C_6H_5) and benzyne (C_6H_4), have been also studied on the Cu(100) surface. They have both dangling bonds that lead to σ bonding with the surface. In phenyl, the π-bonding contribution is important enough to tilt the molecule, whereas for benzyne the molecule stands up on the two unpaired carbon atoms. Benzyne is more strongly bound than phenyl to the surface, but it presents a smaller hydrogen affinity. We conclude that the stability of benzyne on the Cu(100) surface is greater than phenyl, and hence benzyne is the fragment most likely to be found after STM manipulation.

ACKNOWLEDGMENTS

N.L. acknowledges financial support from ACI *Jeunes Chercheurs* and the CNRS program Nano-Objet Individuel. The Center de Calcul Midi-Pyrénées, and the Center d'Informatique National de l'Enseignement Supérieur are gratefully acknowledged for allocation of computing

resources. This work was supported by the EPSRC, the University of Birmingham, and the EU Research-Training Network on Atomic and Molecular Manipulation. M.P. is grateful for support by the Swedish Research Council (VR) and the Swedish foundation for strategic research (SSF) through the materials consortium ''ATOMICS.'' Allocation of computer resources through the Swedish National Allocations Committee (SNAC) is also gratefully acknowledged.

*Corresponding author. Email address: lorente@irsamc.ups-tlse.fr

[1] L.J. Lauhon and W. Ho, J. Phys. Chem. A **104**, 2463 (2000); Surf. Sci. **451**, 219 (2000).
[2] A. Ulman, *An Introduction to Ultrathin Organic Films* (Academic, Boston, 1991).
[3] R. Maboudian, Surf. Sci. Rep. **30**, 207 (1998).
[4] P.A. DiMilla *et al.*, J. Am. Chem. Soc. **116**, 2225 (1994).
[5] O. Chailapakul, L. Sun, C. Xu, and M.R. Crooks, J. Am. Chem. Soc. **115**, 12459 (1993).
[6] J.R. Lomas and G. Pacchioni, Surf. Sci. **365**, 297 (1996).
[7] L. Triguero, L.G.M. Pettersson, B. Minaev, and H. Agren, J. Chem. Phys. **108**, 1193 (1998).
[8] L. Triguero, Y. Luo, L.G.M. Petterson, H. Agren, P. Väterlein, M. Weinelt, A. Föhlisch, and J. Hasselström, Phys. Rev. B **59**, 5189 (1999).
[9] P.W. Kash, M.X. Yang, A.V. Teplyakov, G.W. Flynn, and B.E. Bent, J. Phys. Chem. B **101**, 7908 (1997).
[10] L.G.M. Pettersson, H. Agren, Y. Luo, and L. Triguero, Surf. Sci. **408**, 1 (1998).
[11] S.J. Stranick, M.M. Kamna, and P.S. Weiss, Science **266**, 99 (1994).
[12] J.R. Lomas, C.J. Baddeley, M.S. Tikhov, and R.M. Lambert, Chem. Phys. Lett. **263**, 591 (1996).
[13] T. Munakata, T. Sakashita, M. Tsukakoshi, and J. Nakamura, Chem. Phys. Lett. **271**, 377 (1997).
[14] T. Munakata, T. Sakashita, and K. Shudo, J. Electron Spectrosc. Relat. Phenom. **88**, 591 (1998).
[15] B.E. Koel, J.E. Crowell, B.E. Bent, C.M. Mate, and G.A. Somorjai, J. Phys. Chem. **90**, 2949 (1986).
[16] A. Clotet, J.M. Ricart, F. Illas, G. Pacchioni, and R.M. Lambert, J. Am. Chem. Soc. **122**, 7573 (2000).
[17] F. Mittendorfer and J. Hafner, Surf. Sci. **472**, 133 (2001).
[18] S. Yamagishi, S.J. Jenkins, and D.A. King, J. Chem. Phys. **114**, 5765 (2001).
[19] A. Nilsson, M. Weinelt, T. Wiell, P. Bennich, O. Karis, N. Wassdahl, J. Stöhr, and M.G. Samant, Phys. Rev. Lett. **78**, 2847 (1997).
[20] M. Weinelt, N. Wassdahl, T. Wiell, O. Karis, J. Hasselström, P. Bennich, A. Nilsson, J. Stöhr, and M. Samant, Phys. Rev. B **58**, 7351 (1998).
[21] H. Koschel, G. Held, P. Trischberger, W. Widdra, and H.-P. Steinrück, Surf. Sci. **437**, 125 (1999).
[22] P.S. Weiss, M.M. Kamma, T.M. Graham, and S.J. Stranick, Langmuir **14**, 1284 (1998).
[23] B.E. Bent, Chem. Rev. (Washington, D.C.) **96**, 1361 (1996).
[24] N. Lorente and M. Persson, Faraday Discuss. **117**, 277 (2000).
[25] F.E. Olsson, N. Lorente, M. Persson, L.J. Lauhon, and W. Ho, J. Phys. Chem. B **106**, 8161 (2002).
[26] DACAPO is available at http://www.fysik.dtu.dk/CAMPOS.
[27] G. Kresse and J. Hafner, Phys. Rev. B **47**, 558 (1993).
[28] G. Kresse and J. Furthmueller, Comput. Mat. Sci. **15**, 6 (1996).
[29] M.C. Payne, M.P. Teter, D.C. Allan, T.A. Arias, and J.D. Joannopoulos, Rev. Mod. Phys. **64**, 1045 (1992).
[30] D. Vanderbilt, Phys. Rev. B **41**, 7892 (1990).
[31] J. Tersoff and D.R. Hamman, Phys. Rev. Lett. **50**, 1998 (1983).
[32] J. Tersoff and D.R. Hamman, Phys. Rev. B **31**, 805 (1985).
[33] L. Triguero, A. Föhlisch, P. Väterlein, J. Hasselström, M. Weinelt, L.G.M. Pettersson, Y. Luo, H. Agren, and A. Nilsson, J. Am. Chem. Soc. **122**, 12310 (2000).
[34] P. Jakob and D. Menzel, Surf. Sci. **201**, 503 (1988).
[35] M. Dewar and M. Bull, Soc. Chim. Fr. **C79**, 18 (1951).
[36] J. Chatt and L.J. Duncanson, J. Chem. Soc. **1953**, 2939.
[37] P.S. Weiss and D.M. Eigler, Phys. Rev. Lett. **71**, 3139 (1993).
[38] W.A. Hofer, A.J. Fisher, G.P. Lopinski, and R.A. Wolkow, Phys. Rev. B **63**, 085314 (2001).
[39] P. Sautet and M.-L. Bocquet, Phys. Rev. B **53**, 4910 (1996).
[40] G. Held, W. Braun, H.-P. Steinrück, S. Yamagishi, S.J. Jenkins, and D.A. King, Phys. Rev. Lett. **87**, 216102 (2001).
[41] J.I. Pascual, J.I. Jackiw, Z. Song, P.S. Weiss, H. Conrad, and H.-P. Rust, Phys. Rev. Lett. **86**, 1050 (2001).
[42] Ph. Avouris, R.E. Walkup, A.R. Rossi, T.-C. Shen, G.C. Abeln, J.R. Tucker, and J.W. Lyding, Chem. Phys. Lett. **257**, 148 (1996).
[43] G.P. Salam, M. Persson, and R.E. Palmer, Phys. Rev. B **49**, 10 655 (1994).
[44] D. Menzel and R. Gomer, J. Chem. Phys. **40**, 1164 (1964).